Expert Systems with Applications 40 (2013) 866–872

Contents lists available at SciVerse ScienceDirect

Expert Systems with Applications

journal homepage: www.elsevier.com/locate/eswa

Fuzzy diffusion filter with extended neighborhood

Cetin Elmas [a,*], Recep Demirci [b], Uğur Güvenc [c]

[a] Gazi University, Technology Faculty, Electrical-Electronics Engineering Department, Ankara, Turkey
[b] Gazi University, Technology Faculty, Computer Engineering Department, Ankara, Turkey
[c] Duzce University, Technology Faculty, Electrical-Electronics Engineering Department, Duzce, Turkey

A R T I C L E I N F O

Keywords:
Extended neighborhood
Fuzzy similarity
Diffusivity
Image filter

A B S T R A C T

Anisotropic diffusion filters, which are motivated from heat diffusion between mediums, have become a widely used technique in the field of image processing. In the initial proposals of anisotropic diffusion filters, 4-neighborhood values with diffusivity functions are computed independently for each spatial location because of numerical approximation. However, anisotropic diffusion filters could not be used in real-time image and video processing applications because they need diffusivity parameters, which must be specified by users in every sampling period. In this study, a fuzzy adaptive diffusion filter using extended neighborhood without diffusivity functions has been developed. The fuzzy adaptive diffusion filter does not require any parameter chosen by user and therefore they could be employed in real-time applications. In the fuzzy adaptive diffusion filter, a similarity transformation by means of relation matrix and fuzzy logic is carried out. Accordingly, the similarity image, output of transformation, is directly used as a heat diffusion coefficient in the diffusion filter. Results show that the fuzzy adaptive diffusion filter is very efficient for removing noise in image while preserving edges.

1. Introduction

Filtering is one of the most important image processing steps in image analysis. It is desired that smoothing within a region is performed rather than smoothing across the region boundaries in filter applications. Many filtering techniques have been devised for image filtering. The ideas behind the use of the diffusion equation in image processing arise from the use of the Gaussian filter in multi-scale image analysis (Weeratunga & Kamath, 2002). It is an iterative convolution of a noisy image, $I(x,y,0)$ with a Gaussian kernel:

$$G(x,y) = \frac{1}{2\pi\sigma^2}\exp\left(-\frac{x^2+y^2}{2\sigma^2}\right) \tag{1}$$

where σ is filter variance. At the end of convolutions, the noisy image $I(x,y,0)$ is converted into filtered image $I(x,y,t)$ with time, t as shown in Fig. 1.

In 1990, a nonlinear anisotropic diffusion filter was proposed for images instead of iterative convolutions with Gaussian kernel (Perona & Malik, 1990) as follows:

$$\begin{aligned} &\tfrac{\partial I(x,y,t)}{\partial t} = div(c(x,y,t)\nabla I(x,y,t)) \\ &I(x,y,0) = I_0(x,y) \end{aligned} \tag{2}$$

where $c(x,y,t)$ is the diffusion conductance or diffusivity of the image, ∇ is the gradient operator and $I_0(x,y)$ is contaminated image to be filtered. However, there has been a critical problem of the selection of a proper function for the diffusion conductance, $c(x,y,t)$. The main approach has been based on the magnitude of the gradient of the image as follows:

$$c(x,y,t) = g(\|\nabla I(x,y,t\|)) \tag{3}$$

where $g\,(\cdot)$ is called edge stopping function, which is selected as a decreasing function of the gradient of the image. It must have maximum value at constant signal regions $g(0) = 1$ where the gradients are zero and falls to zero at the edges where the gradients are large. As a result of that, the boundaries of objects in the image could be preserved. However, the region borders or edges are not known in advance and the location of the edges in the image must be estimated. This could be achieved by setting the diffusion coefficient to 1 in the inside of each region and 0 at the borders. Perona and Malik (PM) have proposed two different functions for conduction coefficient at their initial studies as:

$$c(x,y,t) = \exp\left(-(\|\nabla I\|/K)^2\right) \tag{4}$$

and

$$c(x,y,t) = \frac{1}{1+(\|\nabla I\|/K)^2} \tag{5}$$

where the constant K is selected by operator. Accordingly, another fundamental difficulty occurs: what is the best or correct value of

* Corresponding author.
E-mail addresses: celmas@gazi.edu.tr (C. Elmas), rdemirci@gazi.edu.tr (R. Demirci), ugurguvenc@duzce.edu.tr (U. Güvenc).

0957-4174/$ - see front matter
http://dx.doi.org/10.1016/j.eswa.2012.05.042

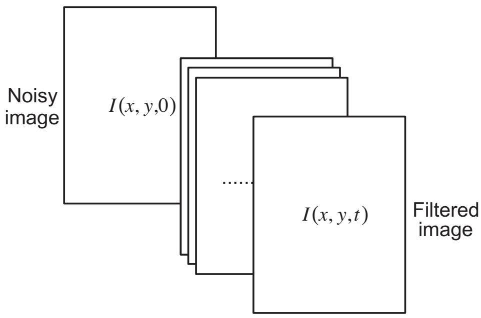

Fig. 1. Filtering process.

K? Therefore the performance of this type of filter will be dependent on the parameter K selected by users. In other words, it will be a user dependent image filter. Therefore the denoising operation is closely related with user experiences. Catte observed some ill-problems with the original functions of Perona and Malik (Catte, Lions, Morel, & Coll, 1992). Following those approaches, several authors have suggested some variations or enhancements of the original functions of Perona and Malik. For example, diffusivity functions suggested by Charbonnier, Feraud, Aubert, and Barlaud (1994) and Weickert, ter Haar Romeny, and Viergever (1998) are based on gradient of image whereas Black et al. proposed an edge stopping function based on robust statistics called Tukey's biweight (Black, Sapiro, Marimont, & Heeger, 1998). Monteil and Beghdadi observed an undesirable effect called "pinhole effect" of original diffusion functions and proposed a different version of diffusion function (Monteil & Beghdadi, 1999). Lu et al. used standard proportional integral derivative (PID) control strategy to minimize mean square error of filtered images (Lu, Shen, & Wang, 2005). Fernandez and Lopez introduced an anisotropic diffusion filter for speckle by means of statistics of noise and signal (Fernandez & Alberola-Lopez, 2006). In addition, different applications of anisotropic diffusion filter were proposed by researchers (Gao, Zhao, Zhang, Zhou, & Huang, 2008; Yu, Wang, & Shen, 2008). The first proposal for anisotropic diffusion filter with fuzzy logic was introduced by Aja et al. in 2001 where absolute differences between central pixel and its neighbor in diffusion direction were used as antecedent and diffusion coefficient was used as consequent in fuzzy reasoning system (Aja, Alborola, & Ruiz, 2001). The fuzzy anisotropic diffusion filter proposed by Aja et al. was improved by Song and Tizhoosh by using wavelet and noise estimators (Song & Tizhoosh, 2006). Recently, Demirci proposed a fuzzy adaptive diffusion filter where the diffusivity parameters for conduction functions were predicted by means of fuzzy rules (Demirci, 2010). The first proposal for diffusion filter with extended neighborhood was done by Barash (2005). The numerical analysis and stability of 8-neighborhood were discussed by Barash in the mentioned study. It was proved that an anisotropic image filter with extended neighborhood could be designed and worked without any stability problem. However, to estimate the diffusion conductance or diffusivity, $c(x, y, t)$, the conventional diffusivity functions were employed. A fuzzy anisotropic diffusion filter without diffusivity functions has been recently introduced by authors (Elmas, Demirci, & Guvenc, 2011; Guvenc, 2008). The diffusion conductance or diffusivity $c(x, y, t)$ of Eq. (2) is directly estimated by using fuzzy rules for 4-neighborhood.

In this study, a fuzzy adaptive diffusion filter with 8-neighborhood has been proposed. In the proposed approach, initially, similarity image, which represents homogeneity of the image to be filtered, was obtained by fuzzy logic. Then, the similarity image is considered as a plate consisting of different materials. While the junction points of materials are dark, internal points or pixels representing the regions are white in similarity image. Then, similarity image was considered as the diffusion conductance or diffusivity, $c(x, y, t)$, of Eq. (2). Consequently, a fuzzy adaptive diffusion filter, which automatically sets its diffusivity without requiring either conduction functions or conduction coefficient, is achieved.

Since the anisotropic diffusion filters need diffusivity parameter, which must be set by operators, they are not suitable for real-time image processing applications because of sampling period in millisecond scales and they work off-line. On other hand, the fuzzy adaptive diffusion filter proposed in this study is fully adaptive and self tuned. It does not require any parameter selected by user. Furthermore, these features introduce possibility of using in real-time.

2. Fuzzy color similarity

An image is a collection of pixels which have feature vectors. The features of a pixel can be a gray level for gray scale images, or red, green, blue levels for color images. The artificial features, which are texture, noise, etc., can also be added into feature vector. In image processing area, the similarity measure of two pixels has been generally assessed so far by means of Euclidian distance in color space. On the other hand, Wuerger, Maloney, and Krauskopf (1995) showed in their research about proximity judgments in color space that perceptual color proximity is not Euclidean in nature. It means that distance information in Euclidean color space is not adequate for similarity judgment. Although the color category map based on fuzzy feature contrast model for image processing applications was constructed by Seaborn, Hepplewhite, and Stonham (2005), the similarity must involve rules and there must be rules for determining a similarity value for any pair of concepts according to Hampton (1998) and the researchers working on the rule-based categorization. With the same approach, a rule-based color similarity was proposed by authors and applied to color image segmentation and filtering (Demirci, 2006; Demirci & Guvenc, 2009). In those studies, similarity of each color component was individually tested and logically merged to build color similarity. The similarity percentage of neighboring pixels including the three components is calculated by means of fuzzy reasoning rules. Gray level differences of each color component between pixel P_1 and P_2 can be stated as follows:

$$\Delta R = |L_{R,1} - L_{R,2}| \tag{6}$$

$$\Delta G = |L_{G,1} - L_{G,2}| \tag{7}$$

$$\Delta B = |L_{B,1} - L_{B,2}| \tag{8}$$

Membership functions for the gray level differences of red, green and blue components as shown in Fig. 2 are defined. Subsequently, gray levels for each color components are partitioned by three linguistic values, which are *Zero*: *ZE*, *Medium*: MD and *Large*: LR. In the same way, the membership functions for similarity of P_1 and P_2 are also defined as shown in Fig. 3. Seven linguistic values

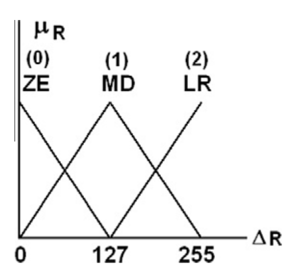

Fig. 2. Membership functions for difference of color components red. (For interpretation of the references to colour in this figure legend, the reader is referred to the web version of this article.)

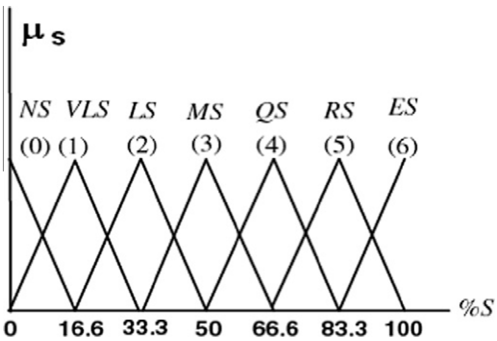

Fig. 3. Membership functions for similarity.

for color similarity are assigned, which are *Not Similar*: *NS*, *Very Little Similar*: *VLS*, *Little Similar*: *LS*, *Medium Similar*: *MS*, *Quite Similar*: *QS*, *Rather Similar*: *QS* and *Exactly Similar*: *ES*.

For a fuzzy system, the mapping of the inputs to the outputs is characterized by a set of *condition-action* rules. The similarity of two pixels in an image can be defined as a system in which there are three inputs and single output. Consequently, linguistic rules for pixel similarity are derived as follows:

Rule1: If ΔR is *Zero* and ΔG is *Zero* and ΔB is *Zero* Then P_1 and P_2 are *Exactly Similar*,
Rule2: If ΔR is *Large* and Δ *G* is *Large* and ΔB is *Large* Then P_1 and P_2 are *Not Similar*,
Rule3: If ΔR is *Large* and Δ *G* is *Zero* and ΔB is *Medium* Then P_1 and P_2 are *Medium Similar*,
Rule4: If ΔR is *Large* and Δ *G* is *Zero* and ΔB is *Zero* Then P_1 and P_2 are *Quite Similar*, so on.

The construction of rules can be in a heuristic way as shown in Table 1. Nevertheless in our case, an automatic method is used. Each input linguistic variables are indexed with 0 for *ZE*, 1 for *MD* and 2 for *LR* whereas the output linguistic variables are indexed from 0 to 6. For each rule, index of membership function for similarity is found as

$$i = 6 - (k + l + m) \tag{9}$$

where *k*, *l* and *m* are index numbers of linguistic variable of each pixel as shown in Table 2.

When the center-average defuzzification and product to represent the conjunctions in the premise are employed, then the similarity percent of P_1 and P_2 could be explicitly represented as:

$$S = \frac{\sum_{j=1}^{Z} S_j \mu_{prem}^j(L)}{\sum_{j=1}^{Z} \mu_{prem}^j(L)} \tag{10}$$

where S_j is center of the similarity percent membership function for the *j*th rule, *Z* is the total number of the rules and $\mu_{prem}^j(L)$ is the certainty of the premise of the *j*th rule given as:

Table 1
Fuzzy rule table for similarity.

μ_B	μ_G	μ_R	μ_s
ZE	ZE	ZE	ES
ZE	ZE	MD	RS
ZE	ZE	LR	QS
.	.	.	.
.	.	.	.
	.	.	.
.			
LR	LR	LR	NS

Table 2
Index table for similarity.

μ_B (k)	μ_G (l)	μ_R (m)	μ_s 6-(*k* + l + *m*)
0	0	0	6
0	0	1	5
0	0	2	4
	.		.
.	.	.	.
.		.	.
	.		
2	2	2	0

$$\mu_{prem}^j(L) = \mu_R^j(L_{\Delta R})\mu_G^j(L_{\Delta G})\mu_B^j(L_{\Delta B}) \tag{11}$$

3. Similarity relation matrix

The similarity of any neighboring two pixels in an image is estimated by means of fuzzy rules as explained in the previous section. Generally, a pixel in an image has eight neighboring pixels as shown in Fig. 4 by considering P_9 is central pixel. Therefore the similarity calculations are performed for all the possible combinations as shown in Fig. 5, and as it was previously done by author Demirci (2007). This approach is well-suited with noisy exemplar approach proposed by authors Kahana and Sekuler (2002) where interstimulus similarity is used to categorize the noisy stimulus. Since interstimulus similarity is a starting point of many cognition theories in terms of physiological studies, the proposed approach is compatible with physiological recognition theories.

By considering Fig. 5, a similarity relation matrix can be assigned as follows:

$$S_{m,n} = \begin{bmatrix} S_{1,1} & S_{1,2} & \cdot & \cdot & S_{1,9} \\ S_{2,1} & S_{2,2} & \cdot & \cdot & S_{2,9} \\ \cdot & \cdot & \cdot & \cdot & \cdot \\ \cdot & \cdot & \cdot & \cdot & \cdot \\ S_{9,1} & S_{9,2} & \cdot & \cdot & S_{9,9} \end{bmatrix} \tag{12}$$

The similarity relation matrix is symmetric. When all elements of the $S_{m,n}$ except diagonal elements are unity, it means that the central pixel and its all neighbors have the same color level or it is perfectly smooth. The local homogeneity of *k*th pixel can be estimated as follows:

$$S_k = \frac{1}{8}\sum_{n=1}^{9} S_{k,n} \quad k \neq n \tag{13}$$

As could be seen from Eq. (12) and Fig. 5, there is no need to consider the self similarity of any pixel. Therefore Eq. (13) gives how the *k*th pixel in mask is similar to the others in average. Although the Eq. (13) gives local average similarity of any pixel, global average similarity of mask shown in Fig. 4 can be estimated by using local average similarities. Consequently, the similarity image is

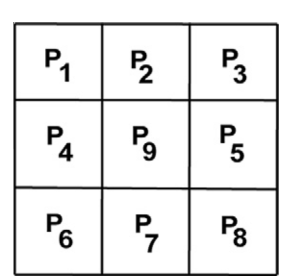

Fig. 4. Neighboring pixels in image.

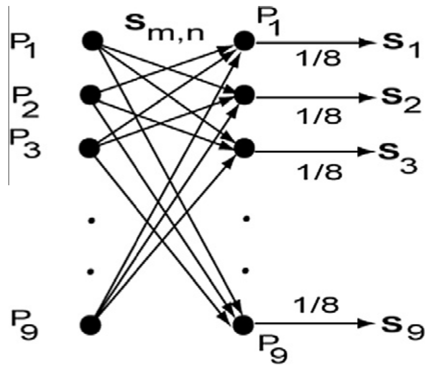

Fig. 5. Similarity network.

obtained. The proposed similarity algorithm was firstly tested with well known cameraman image shown in Fig. 6(a) and fuzzy similarity image shown in Fig. 6(b) was obtained. Then the algorithm was tested with Lena image shown in Fig. 7(a) and fuzzy similarity image shown in Fig. 7(b) was obtained.

4. Fuzzy diffusion filter with extended neighborhood

For traditional anisotropic diffusion filter, the 4-nearest–neighbors discretization of Eq. (2) was proposed by Perona and Malik as follows:

$$I_{i,j}^{t+1} = I_{i,j}^{t} + \lambda[c_N d_N + c_S d_S + c_E d_E + c_W d_W]_{i,j}^{t} \tag{14}$$

where $0 \leqslant \lambda \leqslant 1/4$ for the numerical scheme to be stable, N, S, E, W are subscripts for North, South, East and West respectively. The symbol d indicates nearest–neighbors differences and c is the conduction coefficients in each diffusion direction as shown in Fig. 8(a). On the other hand, different approaches for extension of neighborhood have been proposed (Barash, 2005; Kim, Yoo, Park, Dinh, & Lee, 2007; Li, Wang, & Bao, 2009; Mittal, Kumar, Saxena, Khandelwal, & Kalra, 2010; Zhi & Wang, 2008). For instance, Barash presents an extension to conventional 4-neighborhood directions by adding four new neighborhoods directions. In Barash's discretization approach shown in Fig. 8(b), diagonal edges (NW, NE, SW, SE) were added to the Perona and Malik method. Thus the 8-nearest–neighbors discretization of Eq. (2) was obtained as follows:

(a) (b)

Fig. 6. Cameraman (a) Original, (b) Fuzzy similarity image.

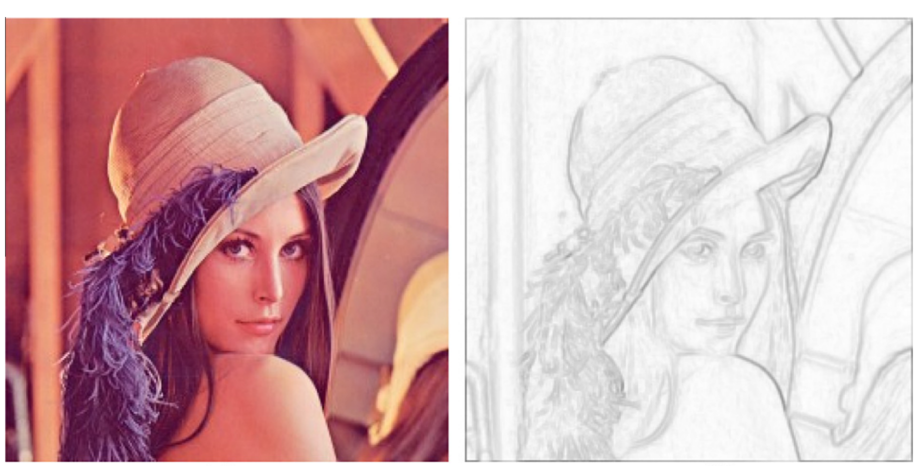

(a) (b)

Fig. 7. Lena (a) Original and (b) Fuzzy similarity image.

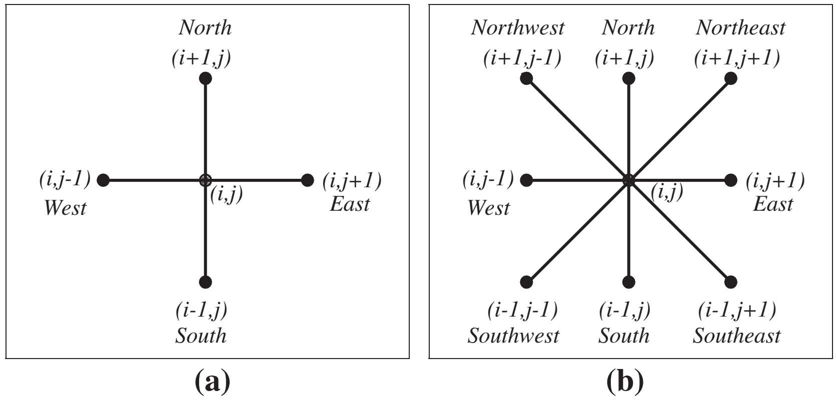

Fig. 8. Structure of discretization (a) 4-nearest-neighbors and (b) 8-nearest–neighbors.

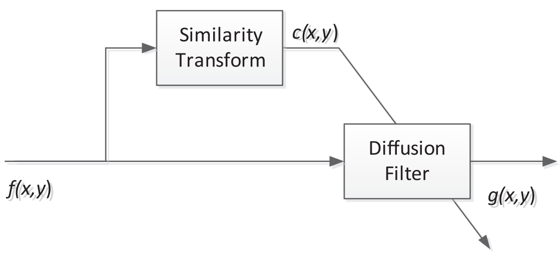

Fig. 9. Fuzzy adaptive diffusion filter.

$$I_{i,j}^{t+1} = I_{i,j}^{t} + \lambda[c_N d_N + c_S d_S + c_E d_E + c_W d_W + c_{NE} d_{NE} + c_{SE} d_{SE} + c_{NW} d_{NW} + c_{SW} d_{SW}]_{i,j}^{t} \quad (15)$$

where $0 \leqslant \lambda \leqslant 1/8$ for the numerical scheme to be stable, NE, SE, NW and SW are subscripts for North-East, South-East, North-West and South-West, respectively. The conduction coefficients in each direction in Eq. (15) change between 0 and 1. If the Figs. 5 and 8(b) are compared, it can be seen that there is matching between local similarities S_k and c, the conduction coefficients in each direction. Also, it is observed that intensity variations or edges in similarity image in Figs. 6(b) and 7(b) is closed to dark, while the homogenous regions are closed to white. In fact, they change from

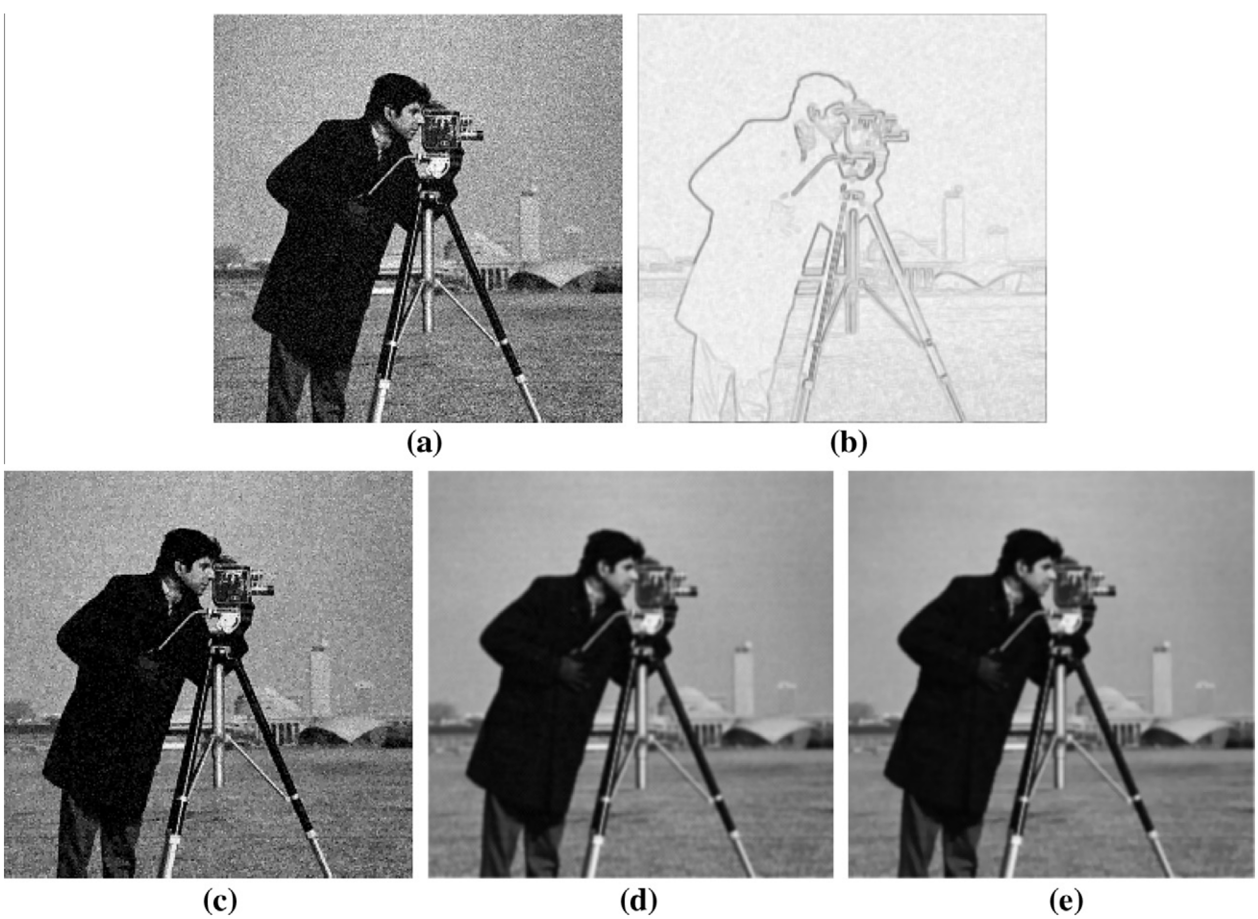

Fig. 10. Cameraman (a) Contaminated with Gaussian noise (b) Fuzzy similarity image: $c(x,y)$ (c) Denoised with PM ($K = 5$) (d) Denoised with FADF (e) Denoised with FADFEN.

Table 3
Results of cameraman image.

Method	MSE	PSNR
PM, $K = 5$	398.362	22.162
FADF	171.878	25.812
FADFEN	**130.068**	**26.989**

0 to 1 according to color variations. Therefore, the similarity image can be interpreted as the diffusion conductance in a metal plate. The dark areas in similarity image are considered as junction points of different materials. Consequently, instead of using the edge stopping function $g(\cdot)$ for the diffusion conductance $c(x,y)$ in Eq. (2), the similarity image is directly assigned as the diffusion conductance $c(x,y)$ for 4-nearest neighbors as:

$$I_{i,j}^{t+1} = I_{i,j}^{t} + \lambda[S_2 d_N + S_7 d_S + S_5 d_E + S_4 d_W]_{i,j}^{t} \tag{16}$$

and it was called fuzzy adaptive diffusion filter (FADF) by the authors (Elmas et al., 2011). By considering numerical approximation of Eq. (2) with extended neighborhood introduced by Barash (2005), the 8-nearest neighborhood extension of FADF can be performed as follows:

$$\begin{aligned} I_{i,j}^{t+1} = I_{i,j}^{t} + \lambda[&S_2 d_N + S_7 d_S + S_5 d_E + S_4 d_W + S_1 d_{NW} + S_3 d_{NE} \\ &+ S_8 d_{SE} + S_6 d_{SW}]_{i,j}^{t} \end{aligned} \tag{17}$$

This novel type of image filter is called fuzzy adaptive diffusion filter with extended neighborhood (FADFEN). As a result, the fuzzy adaptive diffusion filter shown in Fig. 9 was developed. As could be seen, conductivity parameters are estimated from noisy input image by means of similarity transformation and then they are used in the diffusion filter. The gray scale image obtained from this transformation will be dependent on the input image to be filtered. If there is no noise in it, the output image will produce edge information. On the other hand, if the input image is degraded by noise, the output image will show not only edges but also noise information. It will work as a kind of noise estimator as well.

5. Simulation results and discussion

To test the performance of the proposed algorithm, firstly, the cameraman image was contaminated with Gaussian noise as shown in Fig. 10(a) and fuzzy similarity image shown in 10(b) was obtained. Then the noisy image was filtered with conventional diffusion filter with Eq. (4) by the setting conduction coefficients to 5. The iteration number, t was selected as 10 for all experiments. The result obtained with PM filter is shown in Fig. 10(c). In the proposed algorithm, similarity image as shown in Fig. 10(b) was considered as the diffusion conductance $c(x,y)$ for Eq. (2). Filtering performances of FADF and FADFEN are shown in Fig. 10(d) and (e), respectively. The performance comparison of image filters can be done in different ways. For a subjective comparison, visual judgment is used, while for an objective comparison, the MSE is used. The MSE is given by

$$MSE = \frac{1}{MN}\sum_{i=0}^{M-1}\sum_{j=0}^{N-1}(f(x_i,y_j) - g(x_i,y_j))^2 \tag{18}$$

where $f(x,y)$ and $g(x,y)$ are the original and the filtered images, respectively. Moreover M and N are the dimensions of the images.

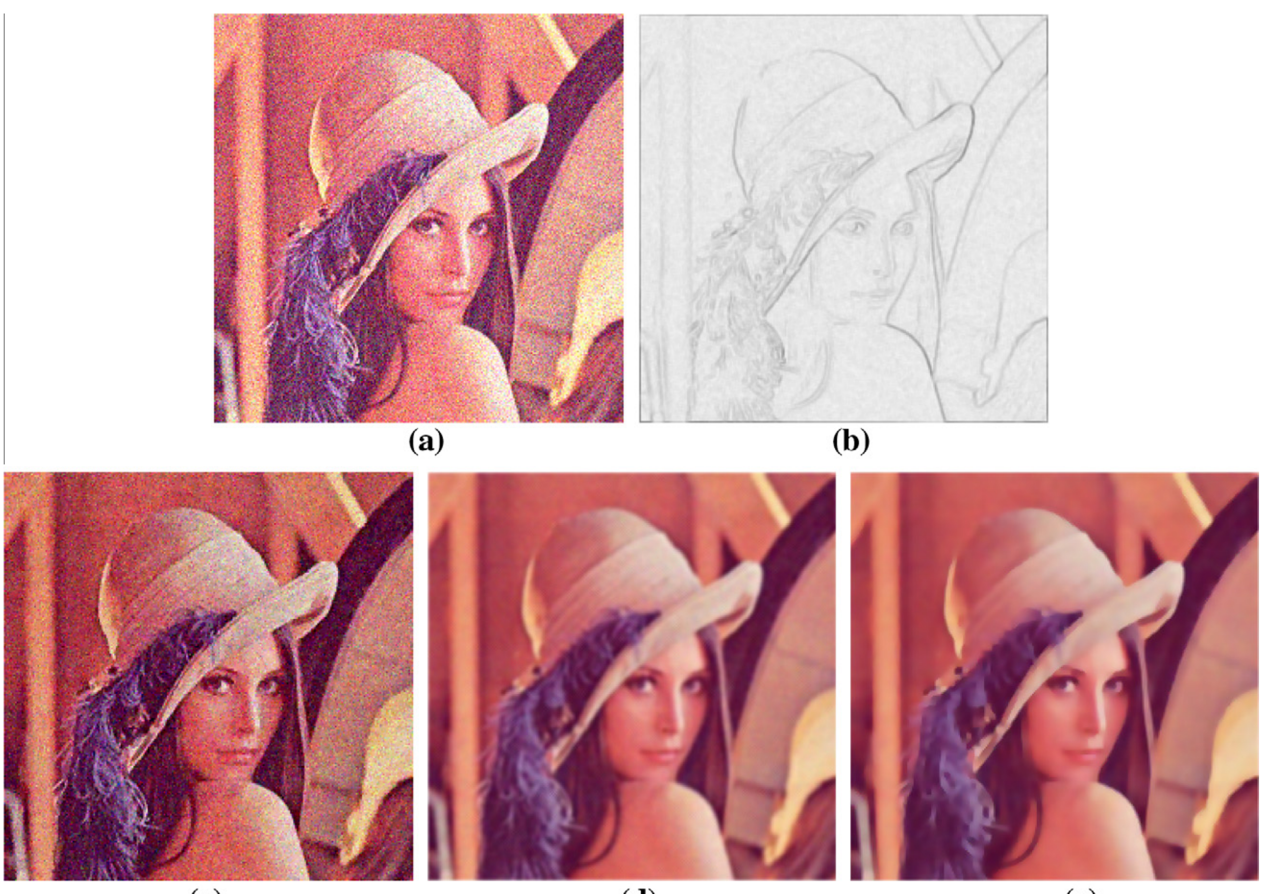

Fig. 11. Lena (a) Contaminated with Gaussian noise. (b) Fuzzy similarity image: $c(x,y)$. (c) Denoised with PM ($K = 5$) (d) Denoised with FADF (e) Denoised with proposed FADFEN.

Table 4
Results of Lena image.

Method	Red channel		Green channel		Blue channel	
	MSE	PSNR	MSE	PSNR	MSE	PSNR
PM $K = 5$	458.1	21.5	440.4	21.7	474.9	21.3
FADF	141.4	26.4	142.021	26.641	123.6	27.2
FADFEN	**101.8**	**28.0**	**117.4**	**27.4**	**114,2**	**27,5**

Also the noise value of corrupted image is calculated by peak signal-to-noise ratio (PSNR) as follows:

$$\mathrm{PSNR} = 10\log\left(\frac{255 \times 255}{\mathrm{MSE}}\right) \tag{19}$$

The MSE and PSNR values obtained with the cameraman images are given in Table 3 where the advantage of FADFEN is quite obvious. The proposed FADF filter was also tested with color image. Therefore, Lena image was contaminated with Gaussian noise shown in Fig. 11(a) and fuzzy similarity image shown in Fig. 11(b) was obtained with the similarity operator. Then the noisy image was filtered with conventional PM filter with Eq. (4). The results obtained with PM filter with conduction coefficient, $K = 5$ is shown in Fig. 11(c). On the other hand, the filtered image with fuzzy adaptive diffusion filter (FADF) and fuzzy adaptive diffusion filter using extended neighborhood (FADFEN) are shown in Fig. 11(d) and (e) respectively. The MSE and PSNR values obtained with Lena are given in Table 4. As could be seen, the performance of FADFEN is better than that of conventional PM filter and FADF.

6. Conclusion

A novel fuzzy adaptive diffusion filter, which does not require any user support, has been developed. The developed image filter not only works with 4-neighborhood anisotropic diffusion but also does with extended neighborhood. Any color or gray scale image can be transformed into similarity or homogeneity image by means of fuzzy rule. The similarity image, which represents intensity variations between 0 and 1, can be substituted into the diffusion conductance in the diffusion filters. Extra computation load for similarity transformation apart from diffusion filter could be considered as the main drawback of the proposed image filter. As a consequence, a fully adaptive image filter is obtained. It does not require any user supplied parameter, K and diffusivity function like traditional diffusion filters. The user dependency of diffusion filters was eliminated. Also it was confirmed that fuzzy adaptive diffusion filters with 8-neighborhood could be designed without any numerical stability problem. Additionally, one of important achievement of this study is that fuzzy adaptive diffusion filter could be used in real-time image processing applications since it does not require any user involvement.

References

Aja, S., Alborola, C., & Ruiz, A. (2001). Fuzzy anisotropic diffusion for speckle filtering. In *IEEE international conference on acoustics speech, and signal processing* (pp. 1262–1264). Utah, USA.

Barash, D. (2005). Nonlinear diffusion filtering on extended neighborhood. *Applied Numerical Mathematics, 52*(1), 1–11.

Black, M. J., Sapiro, G., Marimont, D. H., & Heeger, D. (1998). Robust anisotropic diffusion. *IEEE Transactions on Image Processing, 7*(3), 421–432.

Catte, F., Lions, P. L., Morel, J. M., & Coll, T. (1992). Image selective smoothing and edge detection by nonlinear diffusion. *SIAM Journal on Numerical Analysis, 29*, 182–193.

Charbonnier, P., Feraud, L. B., Aubert, G., & Barlaud, M. (1994). Two deterministic half-quadratic regularization algorithms for computed imaging. In *Proceedings of ICIP-94, IEEE international conference on image processing* (pp.168–172). Texas, USA.

Demirci, R. (2006). Rule-based automatic segmentation of color images. *AEU – International Journal of Electronics and Communications, 60*(6), 435–442.

Demirci, R. (2007). Similarity relation matrix-based color edge detection. *AEU – International Journal of Electronics and Communications, 61*(7), 469–477.

Demirci, R. (2010). Fuzzy adaptive anisotropic filter for medical images. *Expert Systems, 27*(3), 219–229.

Demirci, R., & Guvenc, U. (2009). Fuzzy filter for color images. In T. Dereli, A. Baykasoglu, I.B. Turksen (Eds.), *Proceedings of first international fuzzy systems symposium* (pp. 365–370). Ankara, Turkey.

Elmas, C., Demirci, R., & Guvenc, U., (2011). Fuzzy anisotropic filter without diffusivity functions. In C. Gokceoglu, H. C. Aladag, A. Akgun (Eds.), *Proceedings of second international fuzzy systems Symposium* (pp. 69–74). Ankara, Turkey.

Fernandez, S. A., & Alberola-Lopez, C. (2006). On the estimation of the coefficient of variation for anisotropic diffusion speckle filtering. *IEEE Transactions on Image Processing, 15*(9), 2694–2701.

Gao, G., Zhao, L., Zhang, J., Zhou, D., & Huang, J. (2008). A segmentation algorithm for SAR images based on the anisotropic heat diffusion equation. *Pattern Recognition, 41*(10), 3035–3043.

Guvenc, U. (2008). Adaptive Image Filter Design. PhD. Thesis., Gazi University, Ankara.

Hampton, J. A. (1998). Similarity-based categorization and fuzziness of natural categories. *Cognition, 65*(2–3), 137–165.

Kahana, M. J., & Sekuler, R. (2002). Recognizing spatial patterns: A noisy exemplar approach. *Vision Research, 42*(18), 2177–2192.

Kim, H. S., Yoo, J. M., Park, M. S., Dinh, T. N., & Lee, G. S., (2007). An anisotropic diffusion based on diagonal edges. In *The ninth international conference on advanced communication technology* (pp. 384–388). Phoenix Park, Korea.

Li, J., Wang, L., & Bao, P. (2009). An industrial CT image adaptive filtering method based on anisotropic diffusion. In *IEEE international conference on mechatronics and automation* (pp. 1009–1014). Jilin, China.

Lu, R., Shen, Y., & Wang, Y. (2005). Novel anisotropic diffusion algorithm based on PID control law together with stopping mechanism. In *27th Annual international conference on of the IEEE-EMBS* (pp. 3402–3405). Shanghai, China.

Mittal, D., Kumar, V., Saxena, S. C., Khandelwal, N., & Kalra, N. (2010). Enhancement of the ultrasound images by modified anisotropic diffusion method. *Medical and Biological Engineering and Computing, 48*(12), 1281–1291.

Monteil, J., & Beghdadi, A. (1999). A new interpretation and improvement of the nonlinear anisotropic diffusion for image enhancement. *IEEE Transactions on Pattern Analysis and Machine Intelligence, 21*(9), 940–946.

Perona, P., & Malik, J. (1990). Scale-space and edge detection using anisotropic diffusion. *IEEE Transactions on Pattern Analysis and Machine Intelligence, 12*(7), 629–639.

Seaborn, M., Hepplewhite, L., & Stonham, J. (2005). Fuzzy colour category map for the measurement of colour similarity and dissimilarity. *Pattern Recognition, 38*(2), 165–177.

Song, J., & Tizhoosh, H. R. (2006). Fuzzy anisotropic diffusion based on edge detection. *Journal of Intelligent and Fuzzy Systems, 17*(5), 431–442.

Weeratunga, S., & Kamath, C. (2002). PDE-based non-linear diffusion techniques for denoising scientific and industrial images: An empirical study. In *Image processing: Algorithms and systems conference, SPIE electronic imaging symposium* (pp. 279–290). San Jose.

Weickert, J., ter Haar Romeny, B. M., & Viergever, M. (1998). Efficient and reliable schemes for nonlinear diffusion filtering. *IEEE Transactions on Image Processing, 7*(3), 398–410.

Wuerger, S. M., Maloney, L. T., & Krauskopf, J. (1995). Proximity judgments in color space: Tests of a Euclidean color geometry. *Vision Research, 35*(6), 827–835.

Yu, J., Wang, Y., & Shen, Y. (2008). Noise reduction and edge detection via Kernel anisotropic diffusion. *Pattern Recognition Letters, 29*(10), 1496–1503.

Zhi, X., & Wang, T. (2008). An anisotropic diffusion filter for ultrasonic speckle reduction. In *The fifth IET visual information engineering 2008 conference (VIE'08)* (pp. 327–330). Xi'an, China.